International Journal of the Physical Sciences Vol. 6(3), pp. 391-401, 4 February, 2011
Available online at http://www.academicjournals.org/IJPS
ISSN 1992 - 1950 ©2011 Academic Journals

Full Length Research Paper

Autonomous unmanned aircraft collision avoidance system based on geometric intersection

B. M. Albaker* and N. A. Rahim

UMPEDAC Research Centre, Malaya University, Kuala Lumpur, Malaysia.

Accepted 22 December, 2010

Autonomous Unmanned Aerial Vehicles (UAVs) are envisioned as an integral part of future urban civil and military applications. Large and small scale UAVs will perform large variety of autonomous tasks. However, the capability of UAVs to navigate completely autonomous in real environment is still in its infancy. Autonomous collision avoidance is a necessary step toward this goal. This paper introduces a new collision avoidance approach based on geometrical intersection method for the estimation of collision risk. The approach forms the last line of defense against air-to-air collisions. When a UAV encounters other aircraft that is estimated to approach closer than the minimum safety margin, the resolution unit will be activated in which the direction commands of each UAV in a conflict will be generated, leading to cooperative maneuvering. UAVs flying in a shared airspace are assumed to be linked by real time data bases to share the information of each other and to send and receive the commanded trajectory maneuvering to apply. The proposed approach acts as a control command filter that issues the safest turn and altitude commands, based on collision potential metric, taking into account the minimum possible flight plan change among the solution set.

Key words: Unmanned aerial vehicles, geometric intersection, conflict detection and resolution, rule based, optimial maneuvering and collision avoidance system.

INTRODUCTION

The importance of UAVs in scientific applications has been thoroughly demonstrated in recent years (DoD, 2010). Interest in unmanned aircraft is growing worldwide. The development and use of unmanned aircraft systems is the next step forward in the evolution of aviation (DoD, 2010; Lancher et al., 2008). Whatever missions are chosen for the UAVs, their number and use will significantly increase in the future. Flying multiple UAVs in the same tactical airspace with manned aircraft presents very challenging problem. These vehicles will in some manner, have to detect and avoid conflicts with other aircraft.

Numerous technologies are being explored in the community to develop a solution for Collision Avoidance System (CAS). The problem is multi-dimensional and needs to be addressed at the system level. Many methodologies and skills are published up to the present addressing the problem based on non-cooperative detection, using radar with cooperative rule based avoidance such as our previous research conducted in (Albaker and Rahim, 2009a, b), finding optimal trajectories by using predictive optimal theories (Chaloulos et al., 2010), probabilistic modeling (Kim et al., 2007), potential field (Tang et al., 2010), and so on. A comprehensive review of these methods can be found in (Albaker and Rahim, 2010).

Some of the existing operational CAS systems in use or have been evaluated in the field for manned aircraft and study conducted to deploy it on UAVs are: Airborne Information for Lateral Spacing (AILS) (Waller and Scanlon, 1996), County Technical Assistance Service (CTAS) (Isaacson and Erzberger, 1997), Ground Proximity Warning System (GPWS) (RTCA, 1976) and its recent enhanced version (EGPWS) (Bateman, 1999), Precision Runway Monitor (PRM) (FAA, 1991), Traffic Alert and Collision Avoidance System (TCAS) (RTCA, 1983, 1997; Ford, 1986, 1990), Traffic and Collision Alert Device (TCAD) (Ryan and Brodegard, 1997), User

*Corresponding author. E-mail: baraamalbaker@ymail.com.

Request Evaluation Tool (URET) (Brudnicki et al., 1997), and a prototype conflict detection system for Cargo Airline Association (Kelly, 1999). The other approaches range from abstract concepts to prototype conflict detection and resolution systems being evaluated and used in laboratories. Some approaches were developed for robotics, automobile or naval applications (Coenen and Smeaton, 1989; Iijima et al., 1991; Taylor, 1990; Chakravarthy and Ghose, 1998), but are still not applicable to aviation (Kuchar and Yang, 2000).

As avionics for unmanned aerial vehicles are becoming more sophisticated and widely developed, new algorithms are continued to develop to make them more operational, allowing cooperative behavior in which inter-agent communication of position, heading, waypoints and proposed trajectories are allowed.

Conflict detection can be defined as a predicted violation of a separation assurance standard (Lancher et al., 2008; Nguyen, 2007). Therefore, if the UAV's protected zone is violated, each UAV should resolve the collision. For the free flight concept, it is very essential task to understand the geometric relations between UAVs in a conflict.

This paper considers a team of cooperative UAVs, linked by real time database such as the utilization of an Automatic Dependent Surveillance Broadcasting (ADS-B); each UAV can fly in three dimensional spaces. The paper proposes a risk assessment metric based on geometric intersection between conflicting UAVs. When a potential conflict along the trajectory exists, the collision avoidance is activated to take the action of filtering the possible trajectories to avoid the conflict and the best option to consider based on optimization problem. After a possible threat is removed, the approach measures the time to intercept and return back to its normal flight plan.

A similar work is conducted in (Nguyen, 2007) based on horizon escape window by finding near optimal safe trajectory among all options defined by all UAVs. Although it seems a promising approach applicable specially for low scale UAVs size, however the approach only rely on constant turn commands in two dimensional space whereas in this work the escape is extended to include in addition to heading, the altitude commands. By this inclusion, the free flight concept is much achievable and thereby the aircraft trajectories are given higher escape maneuvering options in case of complicated encounters scenarios. In addition to that, the algorithm is based on simple risk assessment, geometrical intersection and finding minimum distance between conflicting UAVs whereas in his approach a mathematical intensive calculation is required to compute the risk in all UAVs trajectories in a shared airspace making his algorithm difficult to extend for large scale UAVs and to consider another dimensions.

UAV and its trajectories modeling

Two or more UAVs with their initial setup values toward their goal positions are considered sharing the same airspace. The work utilizes two primary frames: the velocity vector and the local frames. The velocity vector frame is attached to the aircraft center of mass, referenced to the standard body frame. The simulation utilizes standard three degree of freedom equation of motion where the velocity (V), flight path angle (γ), heading (ψ), North, East and Down velocities and positions (V_{NED}, P_{NED}) are the state variables. Such that the state vector of the i^{th} UAV is defined by S^i={v,ψ,γ, V_{NED}, P_{NED}}. The state S^i of UAV_i is updated by the three degree of freedom equations of motion given below:

$$\begin{bmatrix} \dot{V} \\ \dot{\psi} V cos\gamma \\ -V\dot{\gamma} \end{bmatrix} = \frac{\vec{F}^V}{m} + T^{VL}\vec{g}^L \quad (1)$$

$$\left[\frac{dp}{dt}\right]^L = T^{LV}\vec{V}^V \quad (2)$$

Where Ψ is the heading angle of the UAV with respect to the positive north-axis. The point-mass equations of motion are derived with respect to North, East and Down (NED) local coordinate systems from (Zipfel, 2007). T^{VL} is the direction transformation matrix that transforms a vector expressed in local frame into a vector expressed in the aircraft's velocity frame as follows:

$$T^{VL} = \begin{bmatrix} \cos\gamma\cos\psi & \cos\gamma\sin\psi & -\sin\gamma \\ -\sin\psi & \cos\psi & 0 \\ \sin\gamma\cos\psi & \sin\gamma\sin\psi & \cos\gamma \end{bmatrix} \quad (3)$$

In a conflict condition, the Euclidian distance between conflicting aircraft is less than or equal to the protected zones of both UAVs, that is, protected zones overlapped. Aircraft's protected zone is assumed to be of a cylindrical shape; sized by 200 m horizontally and 25 m vertically. This assumption is valid for small sized UAVs with a velocity around 25 m/s. The positions and velocities are assumed to be informed by certain broadcasting air-to air communication systems like ADS-B, and the information from such as GPS is assumed to be quite exact. ADS-B is capable of serving the role of cooperative avionics, since it broadcasts the aircraft position as well as its velocity, identity, type and possibly its intent. Through this technology, the relative distance between conflicting UAVs can be simply obtained. With this relative distance, the conflict condition can be evaluated.

$$R_{rel} = \sqrt{(x_A - x_B)^2 + (y_A - y_B)^2 + (z_A - z_B)^2} \quad (4)$$

Where P_{NA}, P_{EA}, P_{DA}, P_{NB}, P_{EB} and P_{DB} are NED coordinate local frame positions of UAV_A and UAV_B respectively. A constant turn trajectory is the path generated from an initial state S_0, by a constant turn command over a missed distance violation in time segment (T_s). For the purpose of computation and implementation, the Turn Command set (TC) is digitized into a set TC={tc_1… tc_{NT}} of N_T equally spaced values in the interval [$-\psi_{max}$, ψ_{max}]. The set also includes the control command tc=0, which is associated with a straight line trajectory. This implies that N_T should be odd number. Hence, $tc_1=\psi_{max}$, $tc_{NT}=-\psi_{max}$ and $tc_{NT/2}=0$.

Similarly, a constant climb/dive trajectory is the path generated from an initial state S_0, by a constant climb command over a horizon time T_H. Again, Climb Command set (CC) is digitized into N_C equal spaced values between in the interval [-max diving, max climbing]. The set also includes the zero climb command for constant altitude flight. The resultant digitized set CC={cc_1… $cc_{Nc/2}$… cc_{Nc}}. Where cc_1=-max diving, $cc_{Nc/2}=0$ and cc_{Nc}=max climbing.

For each tc∈ TC and cc∈ CC there is an associated CT trajectory. As shown in Figure 1, the set of turn/climb trajectories per UAV is therefore comprised N_{T-1} circular paths with N_{c-1} level climb paths

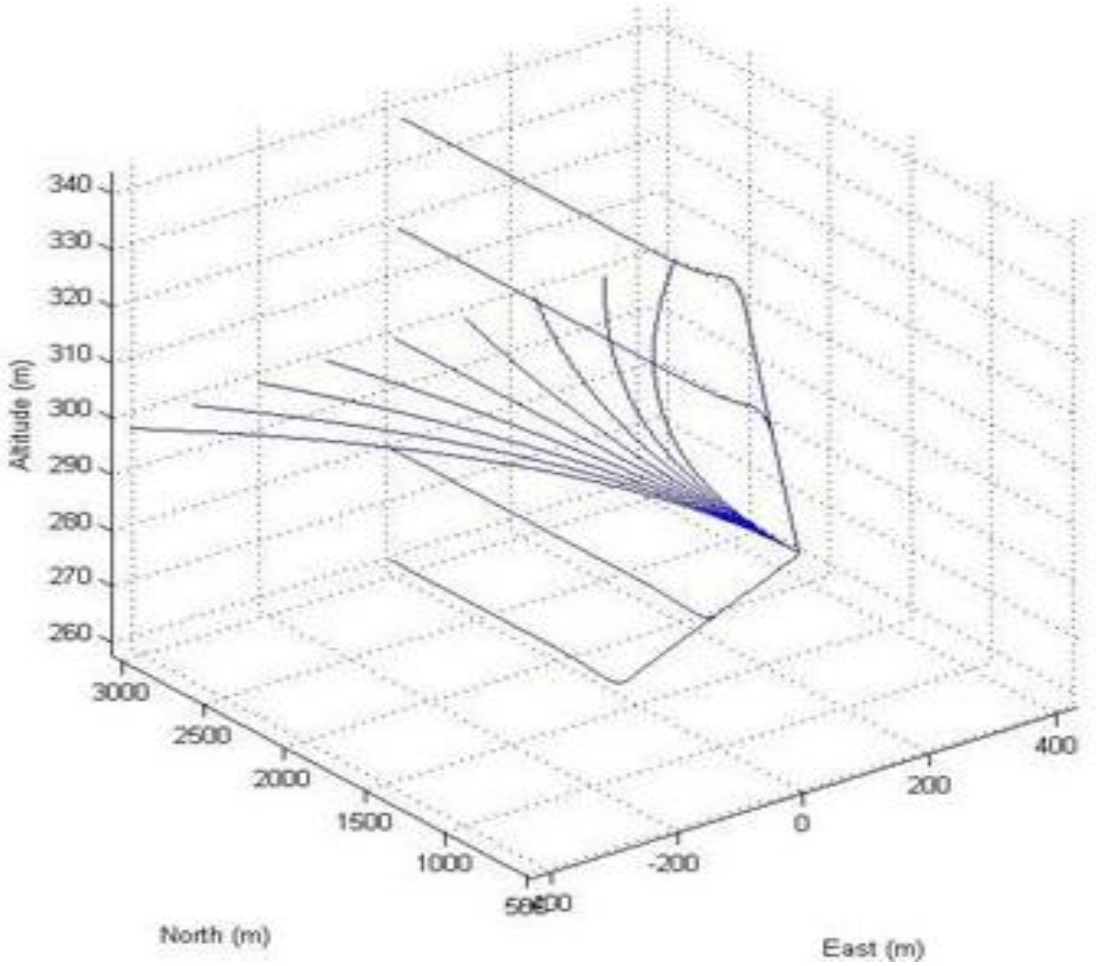

Figure 1. Demonstrates the turn/climb maneuver resolution trajectories in three dimensional local frame.

and one straight path. This leads to TC and CC becoming partitioned into three setsL: TC_L, TC_R and TC_0 and CC_U, CC_D and CC_0 respectively. In such a way, TC_L contains the left positive turning command, TC_R contains the right turning negative commands and TC_0 contains the single straight ahead or zero command. Whereas, CC_U contains the climb up command, CC_D contains the dive down commands and CC_0 contains the single straight zero command.

The time variable $n \in [0,T_s]$ is mapped with the mapping: $M(S,tc,cc,n) \rightarrow (Pn,Pe,Pd)$. Hence, for a given state, S, and turn and climb command, a heading/climbing trajectory in local coordinated frame is given by the set:

$$TJ=\{(Pn,Pe,Pd) \in \mathbb{R}3 | (Pn,Pe,Pd)=M(S,tc,cc,n), \forall n \in [0,T_s]\} \quad (5)$$

Let $TJ^i_{a,b}$ designate the trajectory of the i^{th} UAV associated with the turn command, $tc_a \in TC$ and $cc_b \in CC$, such that:

$$TJ^i_{a,b}=\{(Pn,Pe,Pd) \in \mathbb{R}3 | (Pn,Pe,Pd)=M(S^i,tc_a,cc_b,n), \forall n \in [0,T_s]\} \quad (6)$$

And TJ^i, which designate the set of all trajectories of the i^{th} UAV is given by:

$$TJ^i = \{\cup_{a=1}^{N_T} TJ^i_{a,\frac{N_C}{2}}\} \cup \{\cup_{b=1}^{N_C} TJ^i_{\frac{N_T}{2},b}\} \quad (7)$$

Hence, a trajectory is a geometric object that represents a turn or climb command. The framework of the proposed avoidance method is based upon determining the potential collision for issuing a control command based on the collision potential of flying along the trajectory associated with that control command. The risk assessment of a trajectory is determined by comparing it with trajectories of other UAV agents in a shared airspace.

Risk assessment based on geometric intersection

A trajectory collision risk assessment is a function that assigns a collision potential to a given trajectory using state information of onboard UAV and the states of other UAVs nearby. The purpose of this assessment is to support higher level function on a UAV in determining a course of action control command to avoid potential conflict. To clarify, a UAV will compute the collision potential of own UAV's trajectory with other UAVs trajectories in the vicinity. It is also used to compute the possible trajectories of each UAV for safe paths to follow. These trajectories will be handled by the optimizer unit to compute later the optimum trajectory that a UAV should follow in case possible collision is recorded.

This collision risk metric is a Boolean function that labels a trajectory dangerous if it intersects a trajectory of another UAV, and safe if not.

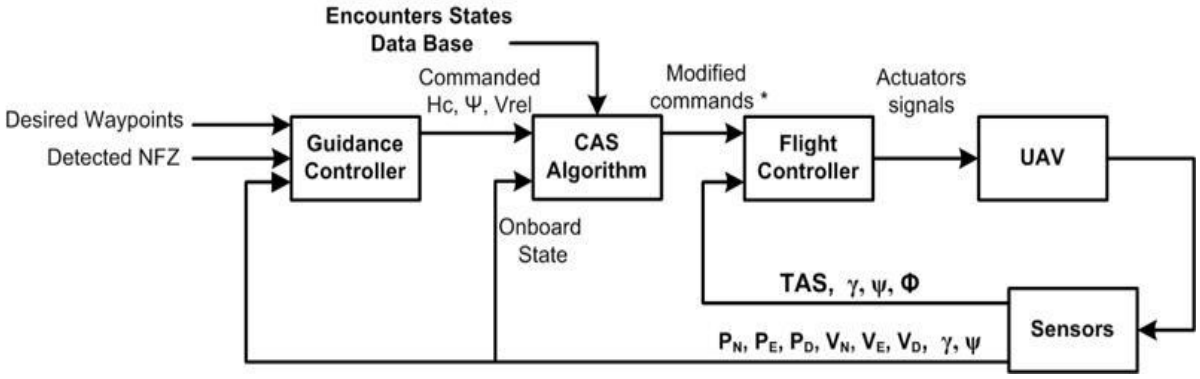

Figure 2. A basic block diagram of complete UAV showing the inputs and outputs to the CAS system.

Let UAV_i be the computing UAV, which is chosen based on the lowest identification number among conflicting UAVs. Let the set of all trajectories of other encounters in the UAV system other than trajectory of UAV_i be represented by:

$$TJ^{i}_{system} = \cup^{N_{UAV}}_{j=1,j\neq i} TJ^{j} \quad (8)$$

The risk metric therefore yields True when the i^{th} UAV's trajectory intersects any trajectory belonging to another UAVs in a shared airspace and yields False if otherwise.

$$Risk\,(TJ^{i}) = (\{TJ^{i} \cap TJ^{i}_{system}\} \neq \{\emptyset\}) \quad (9)$$

The proposed risk metric is based on the computation of the relative distance given in Equation 4, which computes the Euclidean distance between projected future positions of all UAVs starting from their current time and initial positions to the end of the time segment, T_s. Therefore, the metric checks the violation of the relative distance with the horizontal and vertical protected zones of both UAVs in a conflict. If the resultant output returns non-empty values then a conflict is reported along that trajectory. Accordingly the computing aircraft measures the necessary time for the escape and intercept, which depend on the conflict situation among conflicting UAVs. In addition to that, the computing UAV computes the relative collision angle (Φ) at the collision point. These parameters are then passed to the trajectory maneuvering function in which it will handle these parameters to check for available options and choose the best option that leads to a conflict free.

Selection of optimal escape trajectory

The proposed method assumes that the guidance controller is responsible for task execution of the UAV mission. This controller issues commanded relative velocity (Vrel), commanded climb (Hc) and commanded turn (ψ). These outputs are handled by the collision avoidance algorithm to check for potential collision along the trajectory. Accordingly, the collision avoidance system will send the modified commands to the flight controller, which executes those commands by manipulating the control surfaces of the UAV, as shown in Figure. 2.

The control command issued by the collision avoidance system is designated by tc* and cc*. When a UAV's trajectory has zero collision potential, its turn/climb commands should be equal to commanded control values set by the guidance unit. Therefore, choosing a control command, tc∈TC and cc∈CC, that minimizes |ψ - tc| and |Hc - cc| represents the effort towards task execution. These terms represent the cost towards following the guidance commands. Another cost term is added to the optimization problem to account for the collision risk in order to avoid selecting the commands that lead to collision. If there exists trajectories with non-zero collision potential, then the control command is the turn/climb value taken among the set of safest turn/climb values those are closest to the guidance heading and climbing values.

In order to resolve conflict among conflicting aircraft, two sectors around each UAV are identified. According to these sectors the optimum collision free trajectory will be selected. These sectors are defined by the collision angle measured at the first point of protective zone violation. The first sector represents the head-on and rear collision, in which the collision angle, relative to the computing UAV heading, Φ∈[-30º, 30º) for head-on and Φ<-150 or Φ≥150 for rear collision. In this case, the computing UAV will choose an option for the conflicting encounter that deviates at a horizontal distance by the amount equal to the horizontal protected zones of both UAVs. These statements can be encoded as the following optimization problem:

$$tc^{*} = arg\ \min_{tc} k_1|\psi - tc| + Risk(tc, 0) \quad (10)$$

Subjected to:

$tc \in TC_R \cup TC_L$
$\forall n \in [0, T_s]$

Where k_1 is an appropriate small positive number that bound the value of |ψ - tc|.

The second sector represents the right/left side collision, in which the collision angle Φ∈[30º, 150º) for right side collision and Φ∈(-30º, -150º] for left side collision. In this case, the computing UAV will choose an option for the conflicting encounter that deviates at a vertical distance by the amount equal to the vertical protected zones of both UAVs. Again, these statements can be encoded as the following optimization problem:

$$cc^{*} = arg\ \min_{cc} k_1|Hc - cc| + Risk(0, cc) \quad (11)$$

Subjected to:

$cc \in CC_U \cup CC_D$
$\forall n \in [0, T_s]$

Where k_2 is an appropriate small positive number that bound the value of |Hc - cc|. The above equations ensure that both u* and c* are chosen among only the safest turn/climb commands.

Table 1. Simulation parameters.

Simulation parameters	Values
Relative velocity (m/s)	25
Horizontal PZ (m)	200
Vertical PZ (m)	25
Commands update (s)	0.2
Simulation time (min)	4

Table 2. Simulation conditions for the two UAVs scenarios.

UAV states	Computing UAV	Conflicting UAV
First scenario: Head on		
Initial position (Pn: m, Pe: m, Pd: m)	(0,-2000,-300)	(0,2000,-300)
Target position (Pn: m, Pe: m, Pd: m)	(0,4000,-300)	(0,-4000,-300)
Heading angle (º)	90	-90
Second scenario: Side collision		
Initial position (Pn: m, Pe: m, Pd :m)	(0,-2000,-300)	(-2000,0,-300)
Target position (Pn: m, Pe: m, Pd: m)	(0,4000,-300)	(4000,0,-300)
Heading angle (º)	90	0

NUMERICAL RESULTS

Here, the conflict detection and avoidance algorithm previously discussed is evaluated in three sample encounter scenarios to examine the functionality and accuracy of the collision avoidance system. Simulations are executed with initial information about the position and velocity of the UAVs in a conflict. The UAVs are assumed to head towards their goal position and the position and velocity along the path have been treated as broadcast information. The assumptions used and the parameters setup values are given in Table 1.

Two UAVs scenario

The first scenario considers the head-on conflict with the simulation conditions given in Table 2. Both UAVs are on a course that will take them directly to their destinations. A conflict can be easily recognized from Figure 3, where the approaching distance is less than the required separation distance computed from the overlapping of both UAVs' protected zones. Therefore, the conflict risk assessment return true Boolean and activate the avoidance maneuver resolver that in turns find the optimal turn as mentioned in the optimization problem discussed in the previous section. The issued control turn command is depicted in Figure 4. Figure 5 illustrates the escape trajectory system implementation of both UAVs, in NED coordinate, to avoid the potential conflict.

The second scenario considers the right side collision sector with simulation conditions given in Table 2. According to the configuration given in simulation conditions table, a potential collision will be reported as shown in the Figure 6. Relying on Equation 11, the optimizer selects a dive down command for the encounter as a best option to apply. Figure 7 shows the control command issued by the computing aircraft to the conflicting UAV whereas Figure 8 shows how the collision was avoided successfully in side collision scenario.

Four UAVs scenario

This scenario allows multi-collision test at same collision point and time. It is based on the model described in (Hill et al., 2005), which reflects open airspace with no obstacles other than cooperative UAVs. The destinations for these aircraft are the exact opposite side from their operating position with configuration parameters given in Table 3.

In this case, the lower UAV identification number, which is UAV_1, handles all the computations and issues all of the commands to avoid the impending conflict. After detecting the conflict and measuring of colliding parameters, the collision avoidance unit will be invoked to measure the appropriate safe command sate that a conflicting UAV can apply it safely. Relying on Equations 10 and 11, the optimizer selects an option command for each encounter in the shared airspace as a best option to apply. Figure 9 demonstrates the avoidance of the impending conflict in three dimensional NED reference frame. The method proved that by applying the CAS algorithm, the collision will be avoided successfully; satisfying an appropriate separation distance among conflicting UAVs defined by given protected zones of each UAV, as depicted in Figure 10.

The simulation describes a few of the test scenarios used. In these scenarios, the relative distance never invades the minimum separation region. From the simulation, we can see that the horizontal and vertical maneuvers work well.

CONCLUSION

A new collision avoidance method has been developed and simulated. In all test scenarios, the conflict was successfully avoided. Therefore the approach introduced in this paper presents the minimum safety requirement

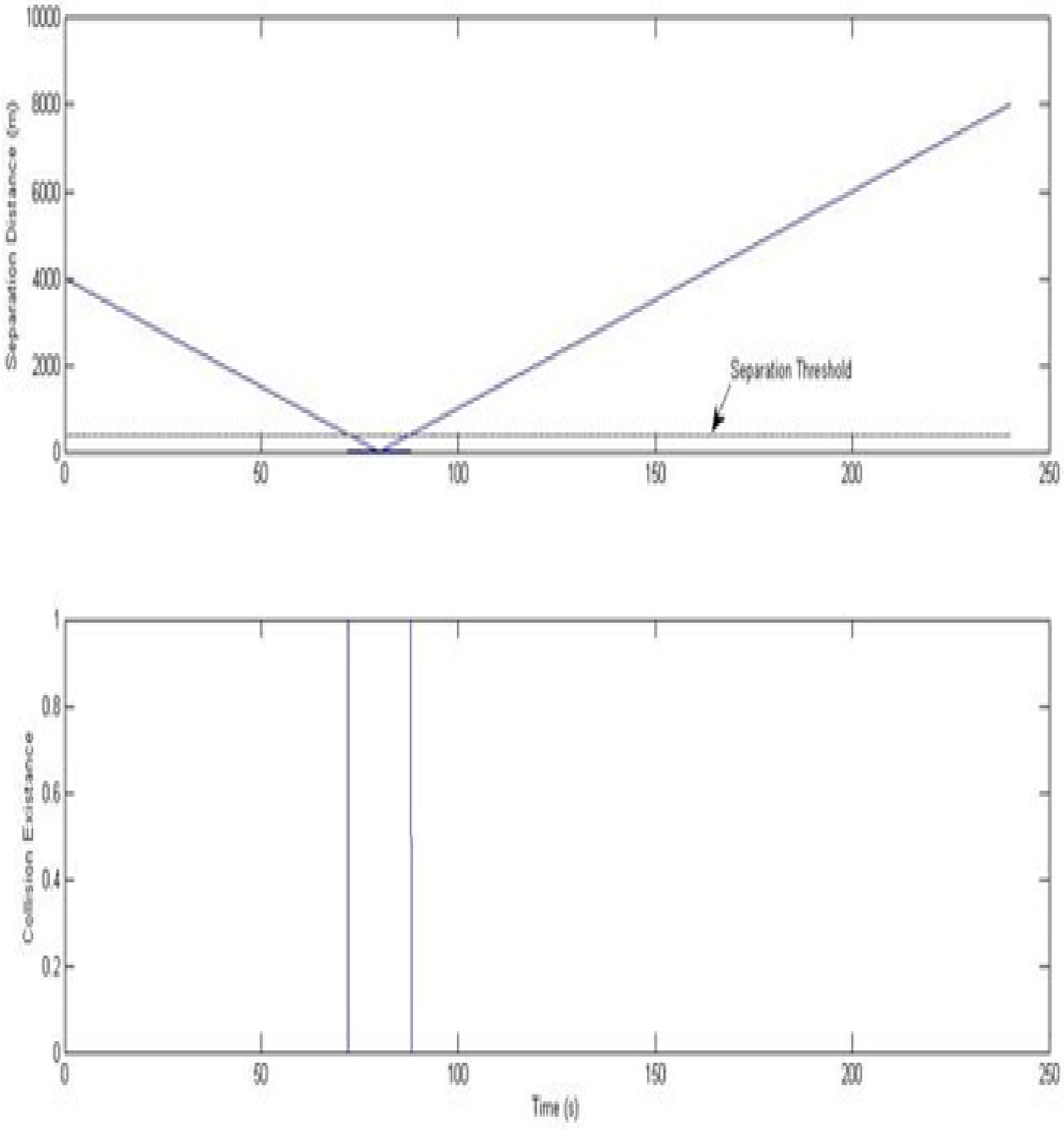

Figure 3. Illustration of head-on collision avoidance scenario showing the separation distance between two UAVs and the collision existence Boolean function for risk assessment.

that should be met. Through the deployment of geometric intersection as collision risk assessment and simple optimization problem for the trajectory escape maneuvering, the conflict resolution maneuver is accomplished successfully. In addition to that, the computation time has been shown to increase linearly

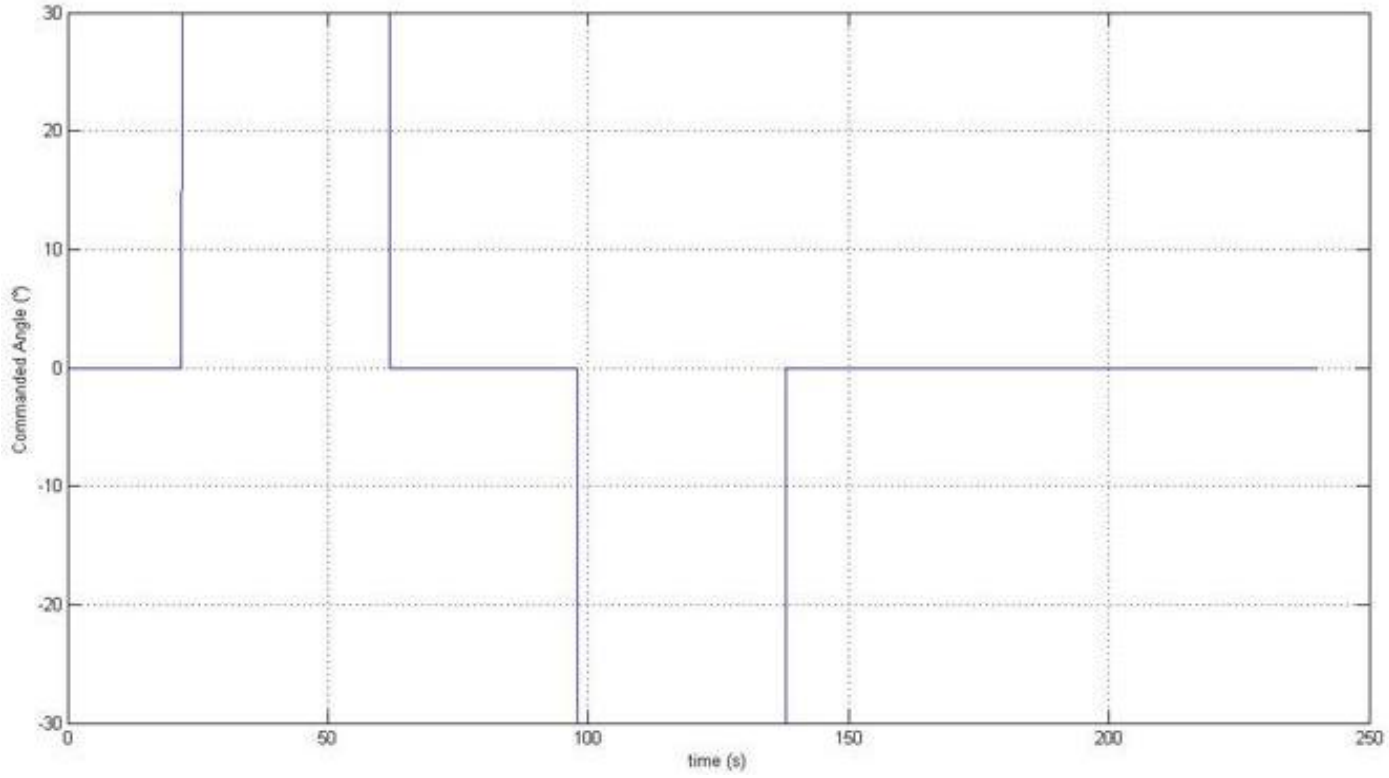

Figure 4. Commanded turn angle issued by the computing UAV.

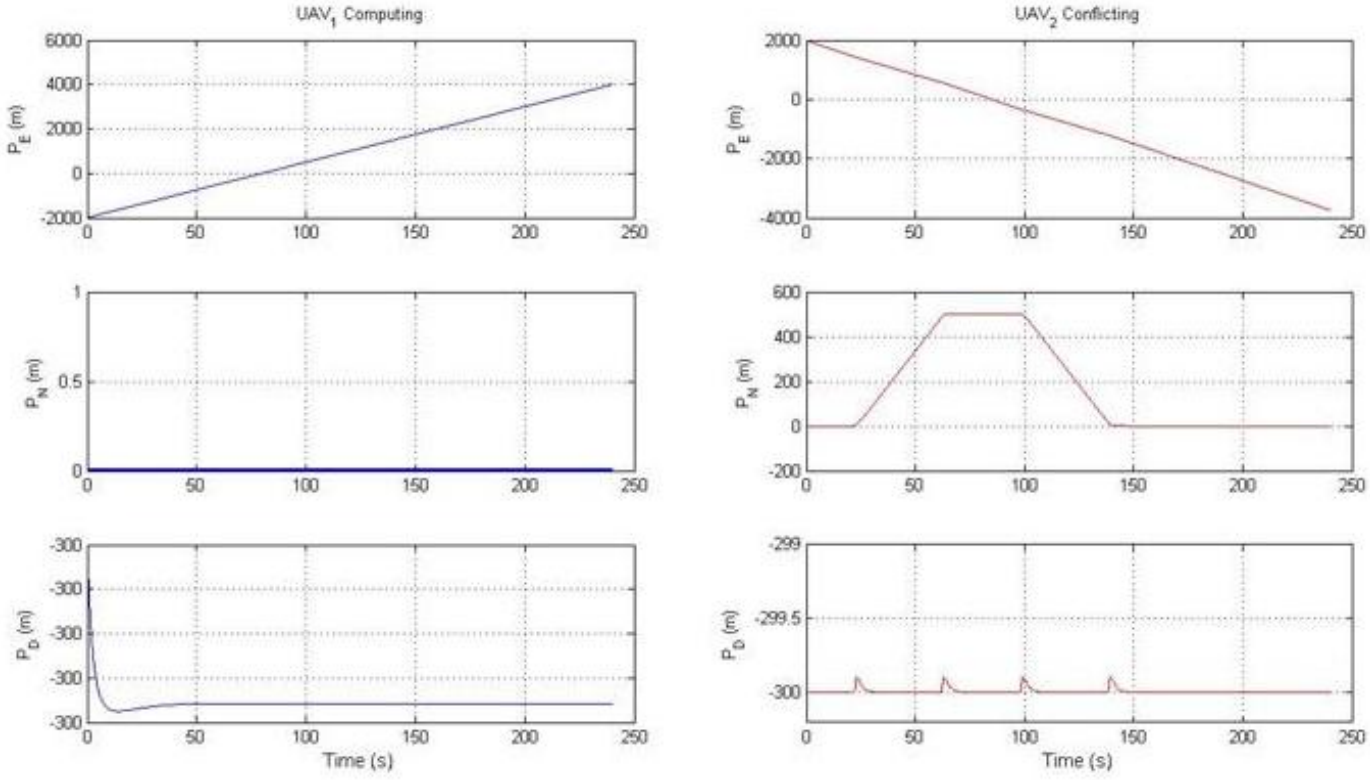

Figure 5. NED positions of the two UAVs after activating the CAS system.

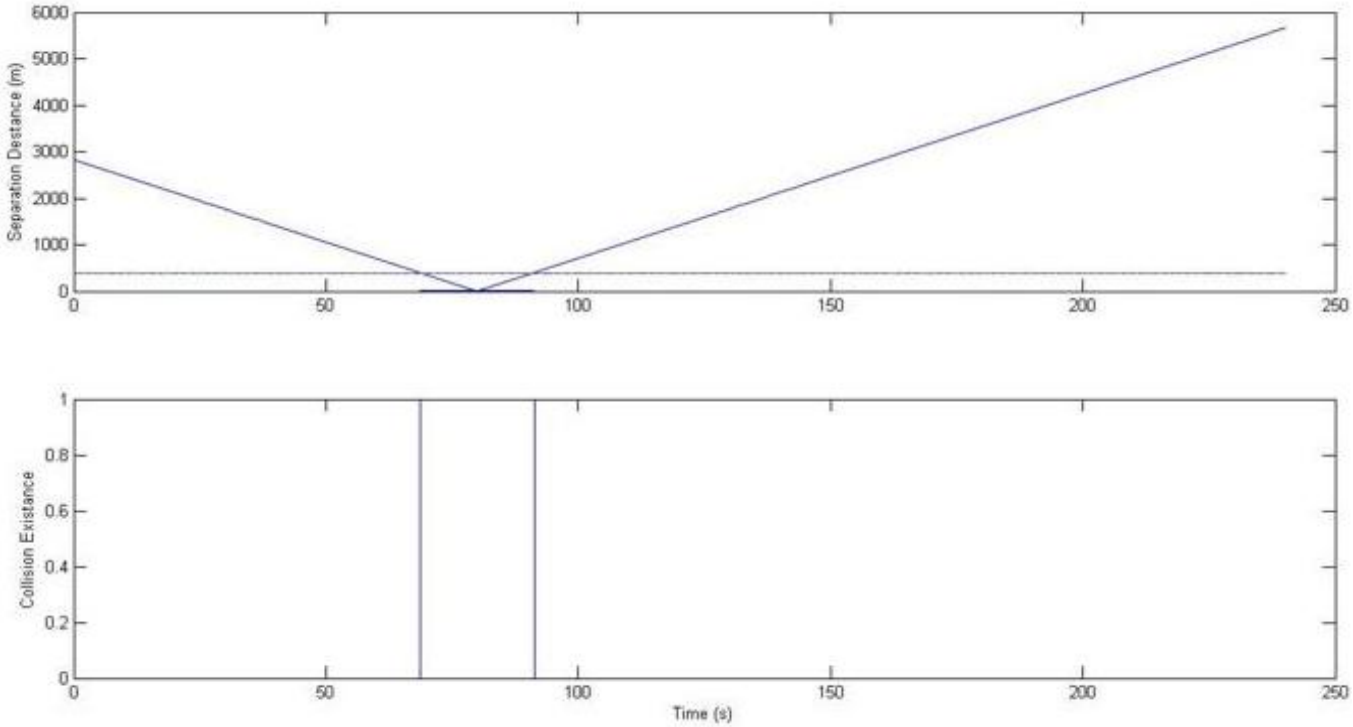

Figure 6. Illustration of right side collision avoidance scenario showing the separation distance violation between the two UAVs and the collision existence Boolean function for risk assessment.

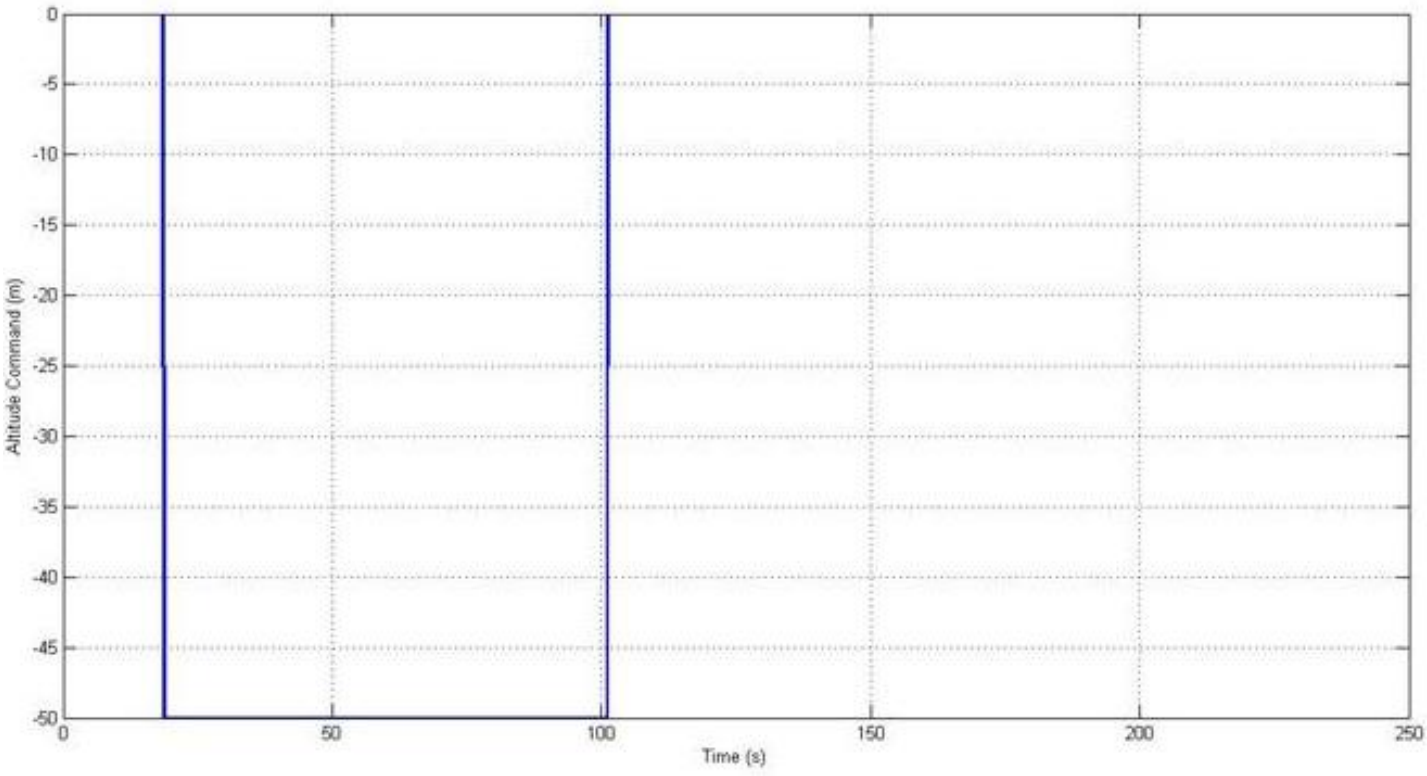

Figure 7. Commanded altitude option generated by the computing UAV as the best option for the conflicting UAV to follow.

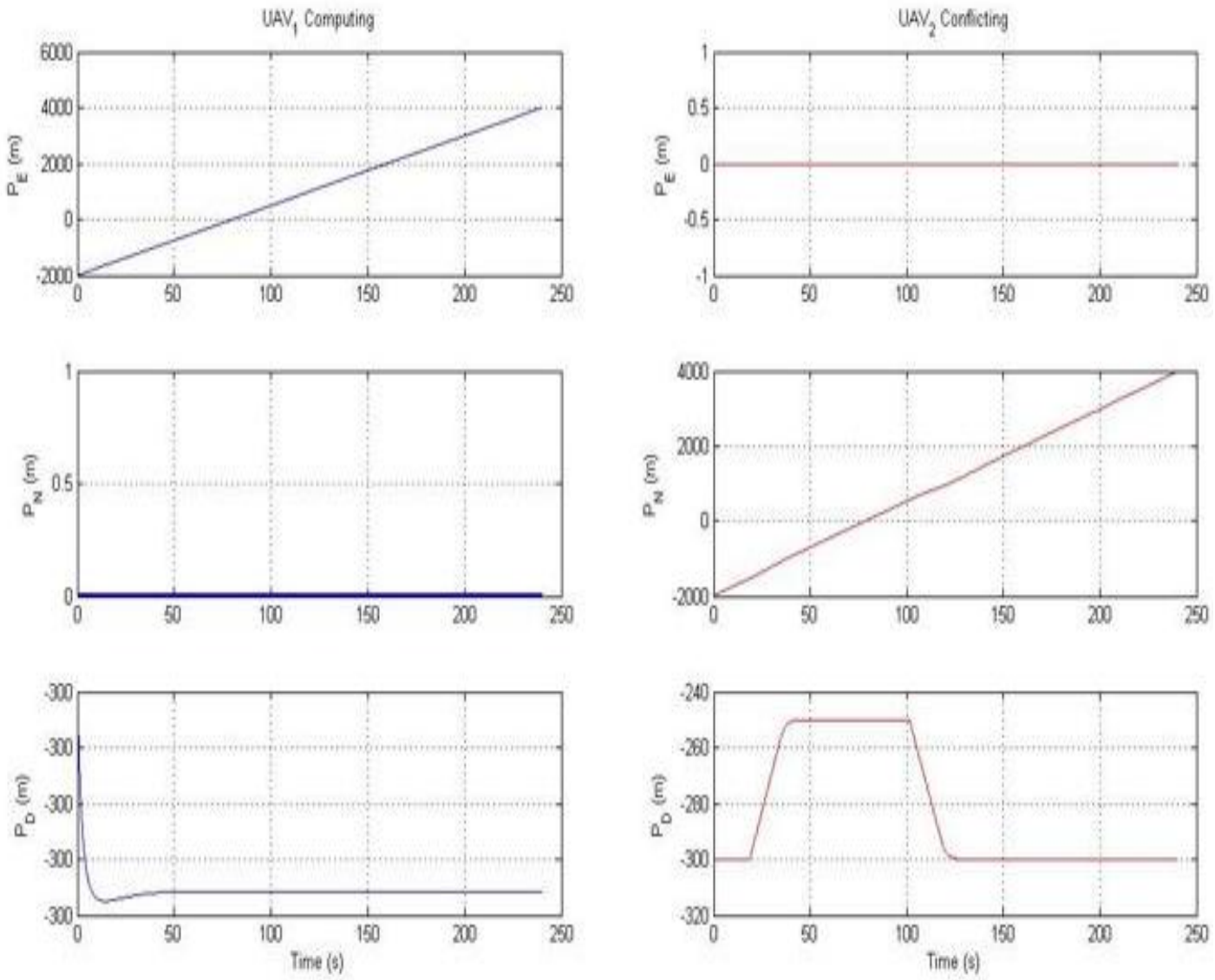

Figure 8. Resolution trajectories in NED coordinate frame of both UAVs after applying the collision algorithm.

Table 3. Simulation conditions for the four UAVs scenario.

UAV states	Computing UAV	Conflicting UAV_1	Conflicting UAV_3	Conflicting UAV_4
Initial position (Pn: m, Pe: m, Pd: m)	(0,-2000,-300)	(0, 2000,-300)	(2000, 0,-300)	(-2000, 0,-300)
Target position (Pn: m, Pe: m, Pd: m)	(0, 2000,-300) (0, 4000,-300)	(0, -2000,-300) (0, -4000,-300)	(-2000, 0,-300) (-4000, 0,-300)	(2000, 0,-300) (4000, 0,-300)
Heading angle (º)	90	-90	180	0

with the number of UAVs in the system, making our approach applicable in time critical situations with an efficient conflict detection and resolution.

The developed collision avoidance system can be integrated with the guidance controller to become a fully functioning autonomous guidance controller. Symmetrical collision scenarios of two UAVs configurations and their waypoints are successfully resolved based on two

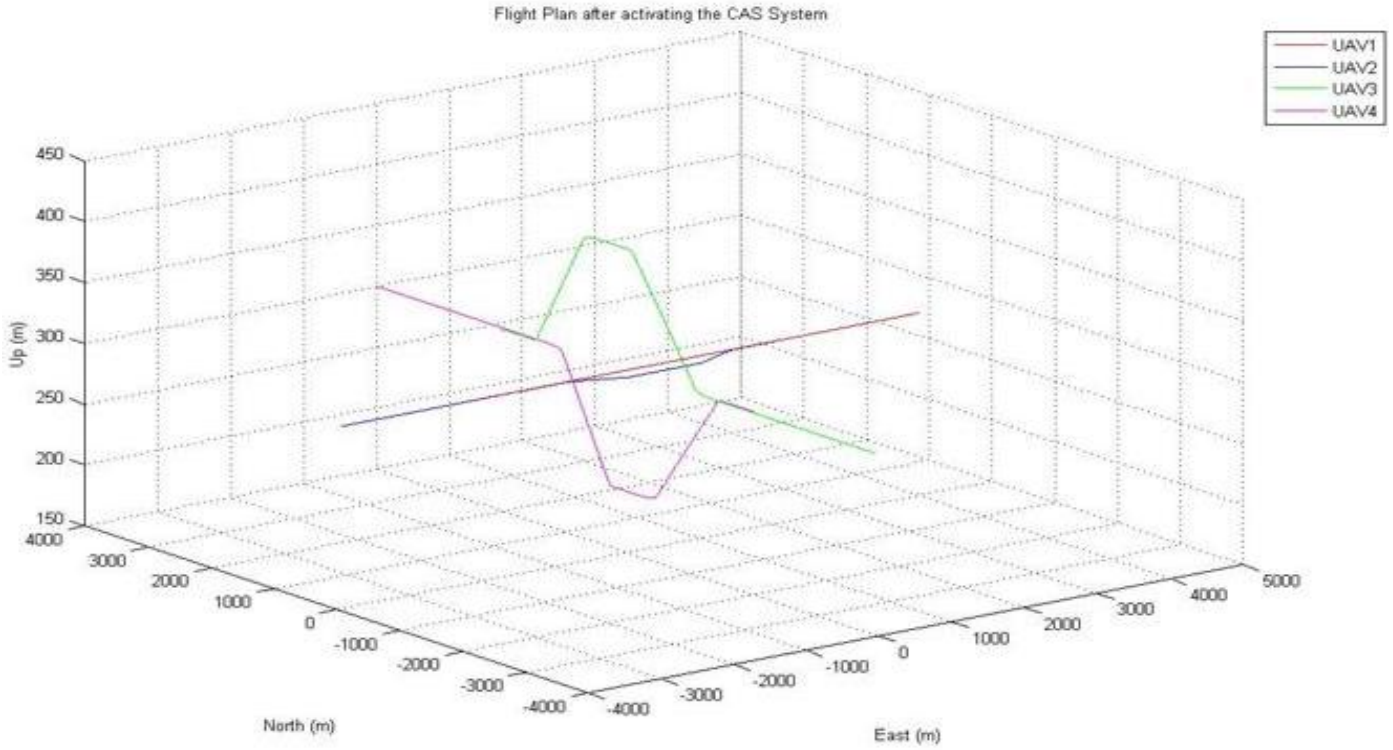

Figure 9. Illustration of avoidance trajectories issued for the four UAVs to escape from potential collision.

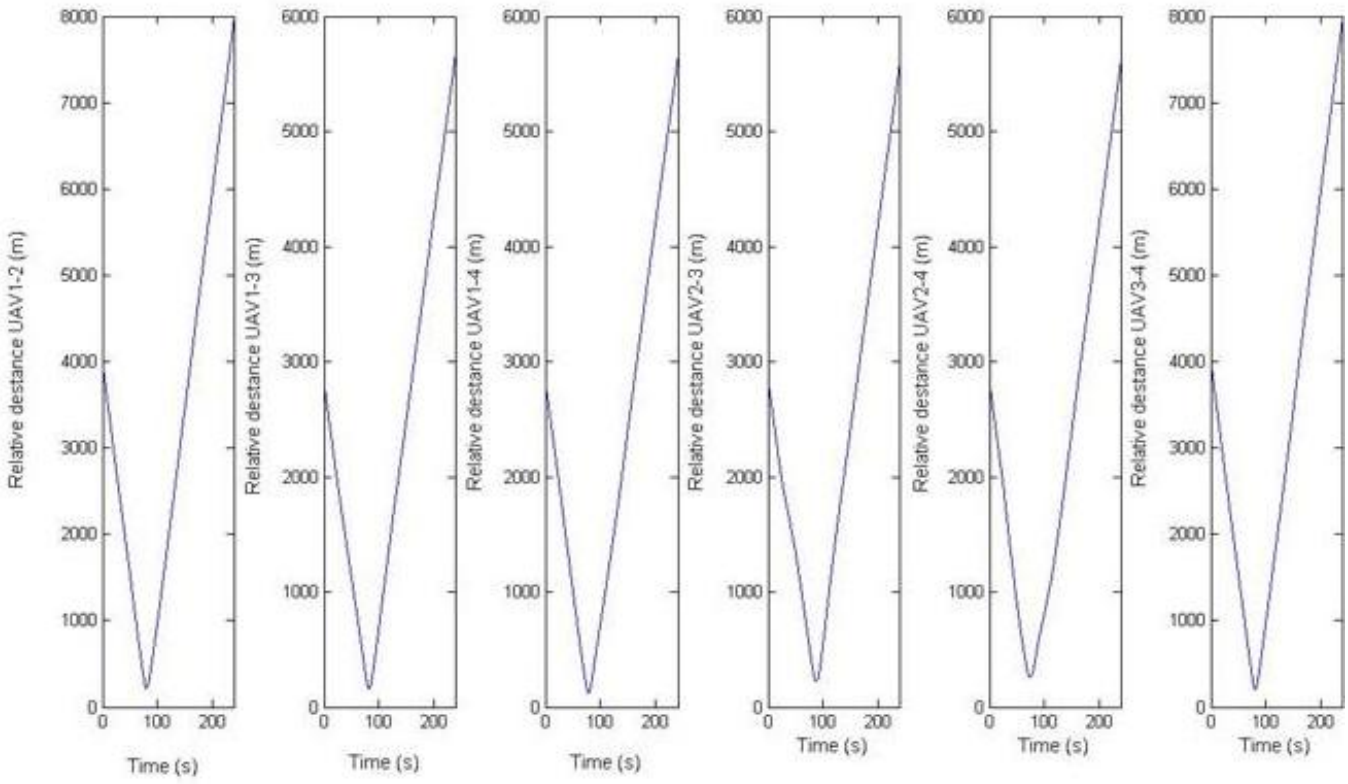

Figure 10. The separation distance among four UAVs after activating CAS system.

resolution logic, altitude and turn commands, and collision free route are applied for both UAVs.

REFERENCES

Albaker BM, Rahim NA (2009). Signal Acquisition and Parameters Estimation of RF Pulse Radars using Novel Method. IETE J. Res., 55(3): 128-134.

Albaker BM, Rahim NA (2009). Straight Projection Conflict Detection and Cooperative Avoidance for Autonomous Unmanned Aircraft Systems. In Proc. 4th IEEE Conf. Ind. Electron. Appl. (ICIEA 2009), Xian P. R. China., pp. 1965-1969.

Albaker BM, Rahim NA (2010). Unmanned Aircraft Collision Detection and Resolution: Concept and Survey. In Proc. 5th IEEE Conf. Ind. Electron. Appl. (ICIEA 2010), Taichung, Taiwan, pp. 248-253.

Bateman D (1999). The Introduction of Enhanced Ground-Proximity Warning Systems (EGPWS) into Civil Aviation Operations Around the World. in Proc. 11th Annu. Eur. Aviation Saf. Semin. (EASS '99), Amsterdam, Netherlands.

Brudnicki D, Lindsay K, McFarland A (1997). Assessment of Field Trials, Algorithmic Performance, and Benefits of the User Request Evaluation Tool (URET) Conflict Probe. In Proc. 16th Digital Avionics Syst. Conf. Irvine, CA, 9: 3-35, 9: 3-44.

Chakravarthy A, Ghose D (1998). Obstacle Avoidance in a Dynamic Environment – A Collision Cone Approach. IEEE Trans. Syst., Man Cybernet., 28(5): 562-574.

Chaloulos G, Hokayem P, Lygeros J (2010). Distributed hierarchical MPC for conflict resolution in air traffic control. In Proc. Am. Control Conf. (ACC), pp. 3945-3950.

Coenen FP, Smeaton GP, Bole AG (1989). Knowledge-Based Collision Avoidance. J. Navigation, 42 (1): 107-116.

Department of Defense (DoD) (2010). U.S. Army Unmanned Aircraft Systems Roadmap 2010-2035. Office of the Secretary of Defense. US Fort Rucker, Alabama.

Federal Aviation Administration (FAA) (1991). Precision Runway Monitor Demonstration Report. Document DOT/FAA/RD-91/5.

Ford R (1986). The Protected Volume of Airspace Generated by an Airbourne Collision Avoidance System. J. Navigation, 39(2): 182-187.

Ford RL, Powell DL (1990). A New Threat Detection Criterion for Airborne Collision Avoidance Systems. J. Navigation, 43(3): 391-403.

Hill J, Johnson F, Archibald J, Frost R, Stirling W (2005). A cooperative multi-agent approach to free flight. In Proc. 4th Int. Joint Conf. Autonom. Agents Multi Agent Syst. Netherlands, pp. 1083-1090.

Iijima Y, Hagiwara H, Kasai H (1991). Results of Collision Avoidance Maneuver Experiments Using a Knowledge-Based Autonomous Piloting System. J. Navigation, 44(2): 194-204.

Isaacson D, Erzberger H (1997). Design of a Conflict Detection Algorithm for the Centre/TRACON Automation System. In Proc. 16th Digital Avionics Syst. Conf. Irvine, CA, pp. 9:3-1, 9:3-9.

Kelly WE (1999). Conflict Detection and Alerting for Separation Assurance Systems. In Proceedings of the 18th Digital Avionics Systems Conference.

Kim K, Park J, Tahk M (2007). UAV Collision Avoidance Using Probabilistic Method in 3-D. In Proc. Int. Conf. Control, Autom. Syst., pp. 826-829.

Kuchar JK, Yang LC (2000). A Review of Conflict Detection and Resolution Modeling Methods. IEEE Trans. Intell. Transportation Syst., 1(4): 179-189.

Lancher AR, Maroney DR, Zeitlin AD (2008). Unmanned Aircraft Collision Avoidance - Technology Assessment and Evaluation Methods. The MITRE Corporation, USA.

Nguyen DL (2007). A Collision Avoidance System using Horizon Escape Windows for Unmanned Aerial Vehicles. MS Thesis, University of California, Berkeley., USA.

Radio Technical Committee on Aeronautics (RTCA) (1976). Minimum Performance Standards -Airborne Ground Proximity Warning Equipment. Document No. RTCA/DO-161A, Washington., D.C.

RTCA (1983). Minimum Performance Specifications for TCAS Airborne Equipment. Document No. RTCA/DO-185, Washington., D.C.

RTCA Special Committee 147 (1997). Minimum Aviation System Performance Standards for Traffic Alert and Collision Avoidance System II (TCAS II) Airborne Equipment. RTCA, RTCA/DO-185A.

Ryan P, Brodegard W (1997). New Collision Avoidance Device is Based on Simple and Passive Design to Keep the Cost Low. Int. Civ. Aviat. Org. ICAO J., 52(4).

Tang L, Dian S, Gu G, Zhou K, Wang S, Feng X (2010). A novel potential field method for obstacle avoidance and path planning of mobile robot. In the proceedings of the 3rd IEEE Int. Conf. Comput. Sci. Inf. Technol. (ICCSIT), pp. 633–637.

Taylor DH (1990). Uncertainty in Collision Avoidance Maneuvering. J. Navigation, 43(2): 238-245.

Waller M, Scanlon C (1996). Proceedings of the NASA Workshop on Flight Deck Centred Parallel Runway Approaches in Instrument Meteorological Conditions. NASA Conference Publ. 10191, Hampton.

Zipfel PH (2007). Modeling and Simulation of Aerospace Vehicle Dynamics, 2nd Edition. American Institute of Aeronautics and Astronautics (AIAA).